Molecular Genetics and Metabolism 147 (2026) 109752

Contents lists available at ScienceDirect

Molecular Genetics and Metabolism

journal homepage: www.elsevier.com/locate/ymgme

Research Paper

From genotype to outcome: Zygosity-specific insights in 63 cases of *CLPB*-related mitochondrial disease

Oliver Heath [a], Francisco Del Caño-Ochoa [b,c], Safa Baris [d], Rosalba Carrozzo [e], David Coman [f], Felix Distelmaier [g], Carolyn Ellaway [h], Rene G. Feichtinger [a], Andrea Finocchi [i], Sergio Guerrero-Castillo [j], Rebecca Halligan [k], Iris Hannibal [l], Amy Kritzer [m], Uta Lichter-Konecki [n], Kajus Merkevicius [o,p], Bianca Panis [q], Robert D.S. Pitceathly [r,s], Chiara Pizzamiglio [r,s], Katarzyna Iwanicka-Pronicka [t], Shamima Rahman [u], Laurie Seltzer [v], Meinolf Siepermann [w], Galit Tal [x], Ron A. Wevers [y], Szymon Ziętkiewicz [z], Santiago Ramón-Maiques [b,c,aa], Johannes A. Mayr [a,1], Saskia B. Wortmann [a,*,1]

[a] *University Children's Hospital, Paracelsus Medical University (PMU), Salzburg, Austria*
[b] *Structure of Macromolecular Targets Unit, Instituto de Biomedicina de Valencia (IBV), CSIC, Valencia, Spain*
[c] *Valencia Biomedical Research Foundation, Centro de Investigación Príncipe Felipe (CIPF), Associated Unit to the Instituto de Biomedicina de Valencia (IBV), Valencia, Spain*
[d] *Marmara University, Division of Pediatric Allergy/Immunology, Istanbul, Turkey*
[e] *Laboratory of Medical Genetics, Translational Cytogenomics Research Unit, Bambino Gesù Children's Hospital, IRCCS, Rome, Italy*
[f] *Metabolic Medicine, Queensland Children's Hospital, Brisbane, Australia*
[g] *Department of General Pediatrics, Neonatology and Pediatric Cardiology, University Children's Hospital, Heinrich-Heine University, Duesseldorf, Germany*
[h] *Genetic Metabolic Disorders Service, Sydney Children's Hospital Network, Randwick, Australia*
[i] *Research Unit of Primary Immunodeficiencies, Immune and Infectious Diseases Division, Academic Department of Pediatrics (DPUO), Bambino Gesù Children's Hospital, IRCCS, Rome, Italy*
[j] *University Children's Research@Kinder-UKE, University Medical Center Hamburg-Eppendorf, Hamburg, Germany*
[k] *Evelina London Children's Hospital, London, UK*
[l] *Division of Pediatric Neurology, Developmental Medicine and Social Pediatrics, Department of Pediatrics, Dr. von Hauner Children's Hospital, Ludwig-Maximilians-University, Munich, Germany*
[m] *Division of Genetics and Genomics, Boston Children's Hospital, Boston, MA, USA*
[n] *Children's Hospital of Pittsburgh, Pittsburgh, PA, USA*
[o] *Clinic of Paediatrics, Institute of Clinical Medicine, Faculty of Medicine, Vilnius University, Vilnius, Lithuania*
[p] *Institute of Biosciences, Life Sciences Center, Vilnius University, Vilnius, Lithuania*
[q] *Department of Pediatrics, MosaKids Children's Hospital, Maastricht University Medical Centre, Maastricht, the Netherlands*
[r] *Department of Neuromuscular Diseases, University College London Queen Square Institute of Neurology, London, UK*
[s] *NHS Highly Specialised Service for Rare Mitochondrial Disorders, Queen Square Centre for Neuromuscular Diseases, The National Hospital for Neurology and Neurosurgery, London, UK*
[t] *Department of Medical Genetics, The Children's Memorial Health Institute, Warsaw, Poland*
[u] *Mitochondrial Research Group, UCL Great Ormond Street Institute of Child Health, and Metabolic Unit, Great Ormond Street Hospital for Children NHS Foundation Trust, London, UK*
[v] *University of Rochester Medical Center, Rochester, NY, USA*
[w] *Department of Paediatric Haematology and Oncology, Children's Hospital Amsterdam Street, Cologne, Germany*
[x] *Metabolic Unit, Ruth Rappaport Children's Hospital, Rambam Health Care Campus, Haifa, Israel*
[y] *Translational Metabolic Laboratory, Department of Human Genetics, Radboud University Medical Center, Nijmegen, the Netherlands*
[z] *Intercollegiate Faculty of Biotechnology, University of Gdansk, Gdansk, Poland*
[aa] *Centro de Investigación Biomédica en Red de Enfermedades Raras (CIBERER)-Instituto de Salud Carlos III, Valencia, Spain*

* Corresponding author at: University Children's Hospital, Paracelsus Medical University (PMU), Müllner Hauptstrasse 48, 5020 Salzburg, Austria.
E-mail address: s.wortmann@salk.at (S.B. Wortmann).
[1] Equal contributions.

https://doi.org/10.1016/j.ymgme.2026.109752
Received 25 November 2025; Received in revised form 22 January 2026; Accepted 22 January 2026
Available online 12 February 2026
1096-7192/© 2026 The Authors. Published by Elsevier Inc. This is an open access article under the CC BY license (http://creativecommons.org/licenses/by/4.0/).

ARTICLE INFO

Keywords:
CLPB
3-methylglutaconic aciduria
Congenital neutropenia
Cataracts
Zygosity
Protein modeling
Ankyrin repeat region
Mitochondrial chaperonopathy
Genotype-phenotype correlation

ABSTRACT

Background: *CLPB*-related mitochondrial disease causes congenital neutropenia, developmental delay/intellectual disability, progressive brain atrophy, movement disorders, cataracts, and 3-methylglutaconic aciduria. Both monoallelic and biallelic forms exist. This retrospective cohort study compared clinical outcomes and genotype–structure–phenotype correlations across zygosity groups.

Methods: Sixty-three individuals (41 biallelic, 22 monoallelic; 6 unpublished) with disease-causing *CLPB* variants were identified via literature review and a multicenter survey. In silico modeling assessed structural impact. A modified CLPB Disease Burden Index (DBI) quantified severity.

Results: Median age at last follow-up was 4.0 years (IQR: 0.25–12.6) in biallelic and 12.0 years (IQR: 5.3–21.0) in monoallelic cases. Death occurred in 66% of biallelic and 23% of monoallelic individuals, with earlier median age at death in biallelic cases (6 months vs 2.4 years). Biallelic cases had significantly higher DBI scores and poorer survival (4-year survival: 50% vs 82%). Stop/stop genotypes were associated with greater disease burden than missense combinations. Structural predictions—particularly variants causing nonsense-mediated decay or ankyrin domain disruption—were stronger survival predictors than zygosity or age of onset. Early-onset disease (<12 months) correlated with more severe progression. Later onset often resulted in milder phenotypes. Hematologic and neurologic features overlapped across zygosity; cataracts and dystonia were more common in biallelic cases. Milestone attainment was poor, with <50% walking or speaking, and only 10–20% doing so on time. Four monoallelic patients received hematopoietic stem cell transplants with mixed outcomes. Granulocyte colony-stimulating factor was associated with improved survival.

Conclusions: This is the largest cohort study to date comparing biallelic and monoallelic CLPB deficiency. Structural variant impact—particularly ankyrin domain disruption—emerged as a key prognostic factor.

1. Introduction

CLPB (also known as Skd3) is a mitochondrial AAA+ (ATPases Associated with Diverse Cellular Activities) protein localized to the intermembrane space. It belongs to the heat shock protein-100 family, a subclass of AAA+ ATPases known for protein disaggregation, although its precise roles in mitochondria remain to be determined [1]. In bacteria (ClpB) and yeast (Hsp104/Hsp78) AAA + -powered disaggregase systems function as molecular chaperones, extracting proteins from their aggregates to rescue folding [2,3]. Similarly, CLPB has been shown to act as an ATP-dependent disaggregase in vitro [4,5]. Compared with canonical AAA+ proteins, CLPB is unique for the presence of an N-terminal Ankyrin-repeat domain preceding its ATPase domain. Structurally, CLPB forms homohexameric rings. This mechanism depends on coordinated conformational changes of individual subunits around the hexameric ring, so that different protomers are in distinct nucleotide and affinity states at any given time, producing directional movement of the substrate. CLPB can also assemble into larger cylindrical dodecameric structures upon substrate binding which are thought to provide a protected environment for client refolding (Fig. 1A) (for review see [1]).

Loss of CLPB function in cell models reduces the solubility of proteins involved in apoptosis, mitochondrial import, calcium handling and respiration [5–7]. Nevertheless, CLPB's role in human disease remains incompletely understood [1]. CLPB interacts with several mitochondrial proteins, including HAX1 and HTRA2, which are linked to disorders that share clinical features with CLPB deficiency. For example, biallelic *HAX1* variants cause *HAX1*-associated severe congenital neutropenia (MIM #610738), characterized by severe neutropenia and -when both isoforms are affected- neurologic involvement [8,9]. Similarly, *HTRA2*-related mitochondrial disease (MIM #617248), like CLPB deficiency, belongs to the growing number of inborn metabolic diseases with 3-methylglutaconic aciduria (3-MGA) as a discriminating feature [10,11], and presents with infantile neurodegeneration, neutropenia, and cataracts [12–14].

CLPB-related disease spans a broad phenotypic spectrum including developmental delay (DD), intellectual disability (ID), epilepsy, movement disorders, neutropenia, cataracts and 3-MGA. First described in 2015 as a condition associated biallelic *CLPB* variants [15–18], subsequent reports identified heterozygous de novo disease-causing variants [19–21]. Clinical severity ranges from isolated neutropenia in some monoallelic cases to pre- or perinatal-onset disease, multisystem involvement and early mortality. Severe neonatal presentations often include hypotonia, spasticity, stimulus-sensitive clonic movements, and progressive brain atrophy, features also recapitulated in zebrafish models [15,17]. However, genotype-phenotype correlations and survival predictors remain poorly defined.

Management remains largely supportive. Granulocyte colony-stimulating factor (G-CSF) is standard therapy for severe neutropenia, with hematopoietic stem cell transplantation (HSCT) considered in refractory cases. Recently, combined uridine-pyruvate supplementation has shown promise in improving oxidative phosphorylation and cell proliferation in fibroblasts derived from patients with mitochondrial disorders [22]. A small clinical study (n = 55) also demonstrated improved lymphocyte counts and T cell proliferation in healthy adults with presumed antibiotic-related mitochondrial toxicity [23].

In this study, we investigate genotype-structure-phenotype correlations in 63 individuals with biallelic and monoallelic *CLPB*-related disease, use structural modeling to interpret variant effects and explore uridine-pyruvate supplementation in three individuals.

2. Subjects and methods

2.1. Study design & data acquisition

This retrospective international cohort study collated de-identified data using a two-step approach (Appendix A: Fig. A1). A PubMed search (conducted in December 2024) was first performed with the terms “CLPB”, “SKD3” or “3-methylglutaconic aciduria type VII”, limited to English-language, full-text human studies. Cross-referencing was undertaken to avoid duplicate inclusion, and overlapping cases were merged. Individuals were eligible for inclusion if they harbored biallelic or monoallelic variants in *CLPB* (RefSeq: NM_030813.6) classified as (likely) pathogenic according to the ACMG/AMP guidelines (Appendix C: Table C4) [24,25].

For previously published cases known to be alive at the time of publication, authors were contacted for follow-up data; if unavailable, only the published information was used. International collaborators contributed new or updated cases using the same electronic case report form (eCRF, Appendix D) as that used for data extraction from the literature. The eCRF captured demographic data, *CLPB* genotype, medical history, survival status, developmental and functional outcomes, neuroimaging and bone marrow findings, and treatment history. To mitigate recall bias, symptom onset was categorized in pre-defined age intervals: 0–28 days, 1–11 months, 1–5 years, 6–12 years, 13–18

years, and > 18 years. Where applicable, symptom severity was classified as mild, moderate, or severe using criteria specified in the eCRF.

2.2. Predicted structural disruption of variants

Nonsense and frameshift variants were evaluated for predicted nonsense-mediated decay (NMD) based on their position using the DECIPHER platform (https://www.deciphergenomics.org/). Missense variants were analyzed in silico for structural impact on the ankyrin repeat region (ANK) or nucleotide binding domain (NBD) of CLPB protein (isoform-1; NP_110440, UniProt: Q9H078–1). Structural predictions integrated crystallographic data (PDBs: 7XBK [26], 7TTS [27]), AlphaFold predicted models of full-length CLPB, and available cryo-electron microscopy density maps (EMD-33106) [28]. Structures were visualized with PyMol (Schrodinger) or COOT [29], and these programs were also used for modeling single nucleotide variants and assessment of their possible structural impact. Figures were prepared with PyMol and ChimeraX [30].

Subjects were stratified by zygosity (biallelic vs. monoallelic), and the variant-type combinations evaluated were limited to stop/stop, missense/missense and missense/stop genotypes in biallelic cases, and missense/wild-type in monoallelic cases. Biallelic genotypes were further classified into the following categories based on predicted structural impact: 1) "NMD-predicted" - both variants predicted to result in NMD; 2) "ANK-disrupting" - at least one allele predicted to affect ANK; and 3) "NBD-disrupting" - either both variants predicted to affect NBD, or one NBD-impacting variant in combination with a predicted NMD allele (Appendix C: Table C1).

2.3. CLPB Disease Burden Index (CLPB-DBI): a cumulative clinical scoring system

To quantify cumulative disease severity, the previous retrospective scoring system [31] was adapted and refined into a 43-point composite score. The CLPB Disease Burden Index (CLPB-DBI) incorporates hematologic, neurologic, and ocular features (cataracts), age at symptom onset (< 12 months vs. later), clinical severity markers (e.g., pregnancy complications, malignancy, developmental regression, hematopoietic stem cell transplant), and survival outcomes (e.g., death in the neonatal period, infancy, or later). A CLPB-DBI calculator is provided in Appendix B, and individual patient DBI scores are detailed in Appendix C: Table C3. Disease severity was stratified as mild (DBI < 10), moderate (DBI 10–24), or severe (DBI ≥ 25) based on clinical review and statistical validation methods that included distributional clustering and Kaplan-Meier survival analysis (Appendix A: Supplementary Results, Fig. A2).

2.4. Statistical analysis

All analyses were performed using R (v12.0 + 467) and GraphPad Prism (v10). Statistical significance was defined as $p < 0.05$. Descriptive statistics are presented as counts (affected / available) and percentages for categorical variables. Group comparisons used Fisher's exact test for categorical variables and Wilcoxon-Mann-Whitney or Kruskal-Wallis tests for continuous variables, with appropriate post hoc corrections.

Power analyses demonstrated >80% power to detect clinically meaningful differences in survival and DBI scores. Survival was analyzed using Kaplan-Meier curves, log-rank tests, and Cox proportional hazards models with Firth's correction for small sample sizes. Individuals reported as alive at last follow-up were treated as censored observations. Missing survival data ($n = 7$ monoallelic cases) were handled conservatively based on sensitivity analyses, as detailed in Appendix A: Supplementary Results [32]. Accordingly, the primary survival analysis incorporated all available patient data using conservative censoring assumptions and provides the most complete and robust estimate of group differences. Disease burden (DBI score) was treated as a continuous outcome and analyzed using robust linear regression, with confidence intervals generated via bootstrapping. Multivariate models included relevant clinical predictors and were refined using backward selection, with model performance assessed by R^2, η^2, and Cohen's f^2.

Developmental skill acquisition was analyzed using inverse Kaplan-Meier methods, scaled to observed rates, with normative milestone limits based on published pediatric standards reported by Feigelman [33]. When age of acquisition was noted to be "age-appropriate", the 50th percentile values (p50) from the Denver Developmental Screening Test II (DDST-II) normative data were used [34].

Exploratory Kaplan-Meier survival analyses were performed to assess variant-specific and GCSF treatment effects, as further detailed in Appendix A: Supplementary Methods.

2.5. Uridine-pyruvate supplementation

In adults treated with mitochondrially toxic antibiotics, combined uridine and pyruvate supplementation exerted a protective effect on immune cells including T cell proliferation, thus providing the rationale for similar supplementation in CLPB deficiency where affected patients are prone to recurrent infections [23]. Three individuals received oral Malto-Uripyr® (Mitobiotix, Italy), a dietary supplement combining uridine-5′-monophosphate (UMP), pyruvate, and the sweetening agent maltodextrin in powder form [35]. Dosing was equivalent to UMP 20–45 mg/kg/day and pyruvate 275–600 mg/kg/day administered in three divided doses [23]. Neutrophil counts as well as frequency of community- and hospital-managed infections were recorded before and during supplementation.

3. Results

3.1. Study cohort and general characteristics

The cohort included 63 individuals (40 female) from 54 families across 18 countries, including six previously unpublished cases (Appendix A: Detailed case reports). Updated clinical data were obtained for 19 of the 57 previously published individuals (Appendix C: Table C2) [15–21,31,36–39]. At the time of analysis, 24 individuals (38%) were alive, and 32 (51%) were deceased, and survival information was unavailable for 7 individuals (11%). These 7 cases were conservatively censored based on predefined sensitivity analysis criteria (Appendix A: Supplementary Results). The cohort comprised 41 individuals with biallelic and 22 with monoallelic *CLPB* variants. Median age at last follow-up was 4.0 years (interquartile range [IQR]: 3 months-12.6 years) in the biallelic group and 12.0 years (IQR: 5.3 years–21.0 years) in the monoallelic group.

3.2. Genotypic spectrum and predicted structural impact of variants

Forty-three unique *CLPB* variants were identified, with no overlap occurring across variant zygosity groups (Table 1).

All variants in monoallelic cases were either missense (n = 11) or small in-frame indels (n = 1). De novo inheritance was confirmed for 10/22 individuals, while family studies were either not available or not reported for the remainder of patients with monoallelic variants. For 12 previously reported individuals without family studies, variant pathogenicity was validated by functional studies [20,21].

Recurrently affected residues in the monoallelic group included Arg561 (Gln/Trp/Gly substitutions; $n = 10$), Gly560 (p.Gly560Arg; $n = 3$) and Arg620 (Cys/His substitutions; $n = 3$), all of which show high evolutionary conservation. The biallelic group exhibited broader genetic diversity, including 19 missense, 7 premature termination codon variants, 2 splice-site variants, 1 indel, 1 insertion, and 1 deletion, with 10 of these variants recurring across unrelated individuals (Fig. 1B).

Six of the seven premature termination codon variants were predicted to trigger nonsense-mediated decay (NMD), based on exon

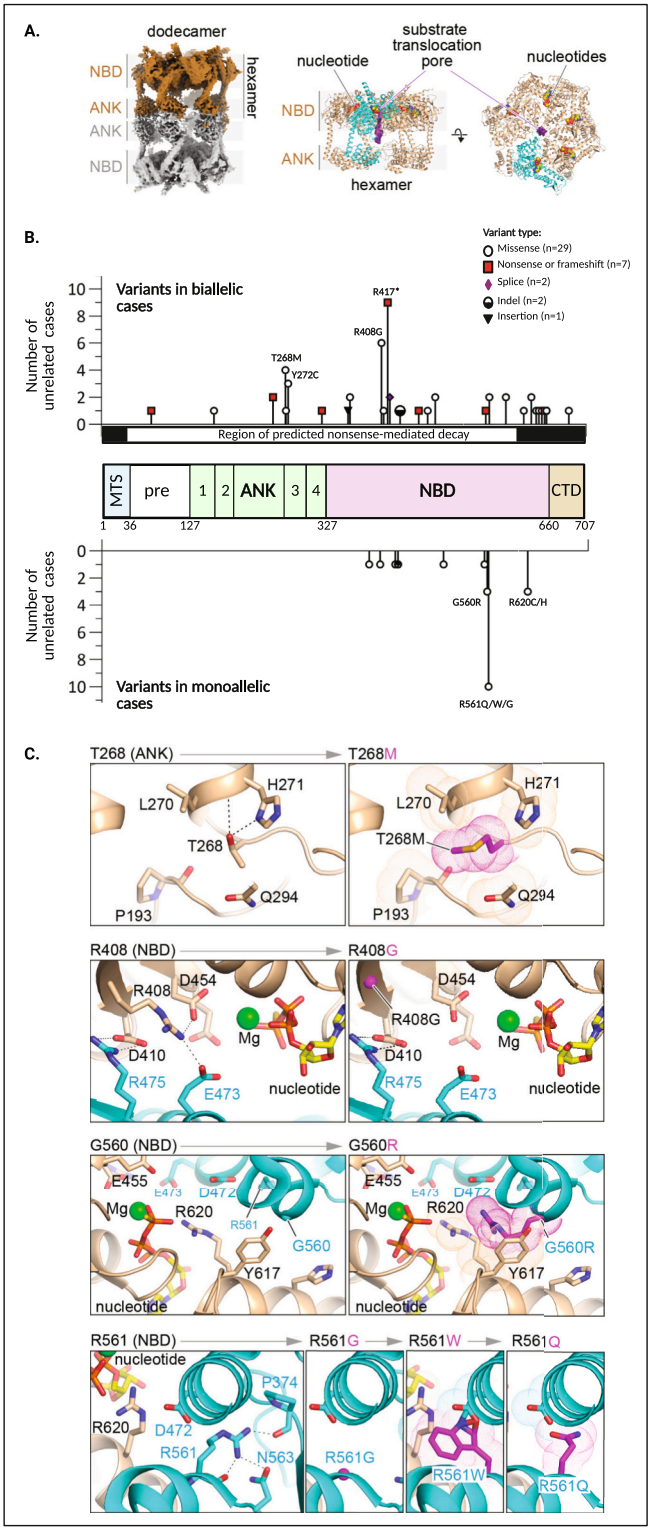

(caption on next column)

Fig. 1. Distribution, structural localization, and predicted effects of CLPB variants.

(A) Structural overview of the CLPB oligomeric complex. Left: cryo-EM density of the CLPB dodecamer (EMD-33106) [29], showing two stacked hexamers colored brown and grey. Middle and right: cartoon representations of the CLPB hexamer in two perpendicular orientations (PDB ID 7TTS) [30], with one monomer highlighted in cyan. The purple density represents a substrate within the central translocation pore. Nucleotides found at the NBD are shown as spheres. ANK and NBD domains are annotated.

(B) Schematic representation of CLPB isoform 1 (NM_030813.6), showing protein domains and the positions of pathogenic variants observed in biallelic (top) and monoallelic (bottom) cases. The Y-axis indicates the number of unrelated individuals carrying each variant. Variants are classified by type: missense, nonsense/frameshift, splice-site, insertion, and indel. Common recurrent variants (found in ≥3 unrelated individuals) are labeled. Domain abbreviations: MTS, mitochondrial targeting sequence; pre, pre-sequence cleaved by PARL at amino acid 127; ANK, ankyrin repeat regions 1–4; NBD, nucleotide-binding domain; CTD, C-terminal domain.

(C) In silico modeling of recurrent missense variants (T268M, R408G, G560R and R561Q/W/G). Left panels: wild-type environment of each mutated position, with key amino acids and the nucleotide shown as sticks, and the Mg^{2+} ion as a green sphere. Dashed lines indicate electrostatic interactions. Right panels: modeled mutant residues, with carbon atoms in magenta. Predicted steric clashes are shown as dot clouds representing atomic radii. For variants near intra-subunit interfaces, adjacent subunits are colored brown and cyan (See Appendix A: Supplementary Results for more details). (For interpretation of the references to colour in this figure legend, the reader is referred to the web version of this article.)

location. Structural analysis suggested that in biallelic cases, missense variants most commonly disrupted the NBD ($n = 18$) or the ANK ($n = 4$), often affecting inter- or intra-subunit interactions (Fig. 1C). In monoallelic cases, all variants affected the NBD ($n = 11$), with the majority (73%, 8/11) predicted to impair ATP binding and/or hydrolysis (Table 1). Three monoallelic variants are located away from the ATP binding site and are predicted to affect NBD intersubunit interactions. Interestingly, while the p.Pro427Leu (in ID1042) and p.Gly429_Tyr430 (in ID1044) de novo variants affect interactions observed between all subunits of the CLPB hexamer, the p.Lys404Thr variant (in ID1063) is only observed forming intersubunit contacts in one of the subunits (Appendix A: Supplementary results).

Based on structural modeling and conservative assumptions regarding variant combination effects, all individuals were classified into one of three structural disruption categories: NMD-predicted ($n = 8$), ANK-disrupting ($n = 10$), or NBD-disrupting ($n = 45$) (Appendix C: Table C1).

3.3. Genotype and predicted structural impact correlate with survival

At data cut-off, 27/41 (66%) biallelic and 5/22 (23%) monoallelic individuals had died. Among these, the median age at death was 6 months (IQR: 1 week-4 years) for biallelic and 2.4 years (IQR: 1.7 years–6.7 years) for monoallelic cases. Causes of death included respiratory failure in 34% (11/32; 9 biallelic, 2 monoallelic), infections in 22% (7/32; 6 biallelic, 1 monoallelic), multiorgan failure in 9% (3/32; 3 biallelic, 0 monoallelic), and malignancy-related complications in 9% (3/32; 2 biallelic, 1 monoallelic), as well as cardiac arrest (1 biallelic) and perforated oesophageal ulcer (1 biallelic).

Survival differed by zygosity ($\chi^2(1) = 8.1$, $p = 0.0045$) (Fig. 2A). Median survival was 4 years in biallelic individuals, while the 4-year survival rate in those with monoallelic variants was 82% (95% CI: 30% - 60%). Survival also differed by age of onset ($\chi^2(1) = 8.5$, $p = 0.0036$), with more deaths reported in individuals with disease onset before 12 months of age (30/50; 60%) vs. later onset (1/13; 8%). When stratifying by zygosity, this remained so among biallelic individuals only ($\chi^2(1) = 9.1$, $p = 0.0025$), where median survival in those with early onset dropped further to 2.5 years (Fig. 2B, Appendix A: Fig. A3a).

Table 1
Genotypic spectrum of 63 individuals with *CLPB*-related mitochondrial disease included in this study.

Variant #	cDNA change (NM_030813.6)	Corresponding protein change	gnomAD v4.1 (ENST00000294053.9) # het | # hom | allele frequency	Cases, n	Zygosity of affected individuals	Predicted structural disruption (based on in silico modeling or variant position)
1	c.216del	p.Arg73Alafs*168	absent	1	biallelic	Nonsense-mediated decay
2	c.491 A > C	p.His164Pro	1 | 0 | 6.20e-7	2	biallelic	ANK domain: disrupted intrasubunit interactions
3	c.748C > T	p.Arg250*	9 | 0 | 5.58e-6	2	biallelic	Nonsense-mediated decay
4	c.803C > T	p.Thr268Met	24 | 0 | 1.49e-5	5	biallelic	ANK domain: disrupted intrasubunit interactions
5	c.805G > A	p.Ala269Thr	absent	1	biallelic	ANK domain: disrupted intrasubunit interactions
6	c.815 A > G	p.Tyr272Cys	5 | 0 | 3.11e-6	3	biallelic	ANK domain: disrupted intrasubunit interactions
7	c.961 A > T	p.Lys321*	absent	1	biallelic	Nonsense-mediated decay
8	c.1079-23 T > A	p.Ala359_Ala360insAspLeuValCysLeuAlaVal	absent	2	biallelic	NBD: disrupted intersubunit interactions
9	Intragenic deletion including exon 9	(includes aa 360–386)	NA	1	biallelic	Nonsense-mediated decay
10	c.1084C > T	p.Arg362Trp	5 | 0 | 3.10e-6	1	biallelic	NBD: disrupted intersubunit interactions
11	c.1085G > A	p.Arg362Gln	13 | 0 | 8.05e-6	1	biallelic	NBD: disrupted inter/ intra-subunit interactions
12	c.1163C > A	p.Thr388Lys	absent	1	monoallelic	NBD: disrupted ATP binding/hydrolysis
13	c.1211 A > C	p.Lys404Thr	absent	1	monoallelic	NBD: disrupted intersubunit interactions
14	c.1222 A > G	p.Arg408Gly	319 | 0 |1.98e-4	7	biallelic	NBD: disrupted intersubunit interactions
15	c.1233G > A	p.Met411Ile	45 | 0 | 2.79e-5	2	biallelic	NBD: disrupted intrasubunit interactions
16	c.1249C > T	p.Arg417*	129 | 0 | 7.99e-5	10	biallelic	Nonsense-mediated decay
17	c.1257 + 5G > T	?	absent	1	biallelic	NBD: exon 11 skipping and in-frame loss of 15 amino acids between Walker A motif and Pore loop
18	c.1257 + 5G > A	?	absent	1	biallelic	NBD: exon 11 skipping and in-frame loss of 15 amino acids between Walker A motif and Pore loop
19	c.1280C > T	p.Pro427Leu	absent	1	monoallelic	NBD: disrupted intersubunit interactions
20	c.1286_1288delinsACA	p.Gly429_Tyr430delinsAspAsn	absent	1	monoallelic	NBD: disrupted intersubunit interactions
21	c.1305_1307inv	p.Glu435_Gly436delinsAspPro	absent	1	biallelic	NBD: disrupted intersubunit interactions
22	c.1383dupA	p.Asp462Argfs*11	25 | 0 | 1.55e-5	1	biallelic	Nonsense-mediated decay
23	c.1424G > A	p.Arg475Gln	17 | 0 | 1.05e-5	1	biallelic	NBD: disrupted intersubunit interactions
24	c.1456 T > C	p.Cys486Arg	absent	2	biallelic	NBD: disrupted intersubunit interactions
25	c.1456 T > C	p.Asn496Lys	absent	1	monoallelic	NBD: disrupted ATP binding/hydrolysis
26	c.1669G > A	p.Glu557Lys	absent	1	monoallelic	NBD: disrupted ATP binding/hydrolysis
27	c.1678G > A	p.Gly560Arg	absent	3	monoallelic	NBD: disrupted ATP binding/hydrolysis
28	c.1681C > T	p.Arg561Trp	absent	3	monoallelic	NBD: disrupted ATP binding/hydrolysis
29	c.1681C > G	p.Arg561Gly	absent	1	monoallelic	NBD: disrupted ATP binding/hydrolysis
30	c.1682G > A	p.Arg561Gln	absent	6	monoallelic	NBD: disrupted ATP binding/hydrolysis
31	c.1685delT	p.Ile562Thrfs*23	absent	4	biallelic	Nonsense-mediated decay
32	c.1700 A > G	p.Tyr567Cys	63 | 0 | 3.90e-5	2	biallelic	NBD: disrupted intrasubunit interactions
33	c.1772C > T	p.Ala591Val	absent	2	biallelic	NBD: disrupted intrasubunit interactions
34	c.1850 A > G	p.Tyr617Cys	4 | 0 | 2.48e-6	2	biallelic	NBD: disrupted intersubunit interactions
35	c.1858C > T	p.Arg620Cys	absent	2	monoallelic	NBD: disrupted ATP binding/hydrolysis
36	c.1859G > A	p.Arg620His	absent	1	monoallelic	NBD: disrupted ATP binding/hydrolysis

(*continued on next page*)

Table 1 (*continued*)

Variant #	cDNA change (NM_030813.6)	Corresponding protein change	gnomAD v4.1 (ENST00000294053.9) # het | # hom | allele frequency	Cases, n	Zygosity of affected individuals	Predicted structural disruption (based on in silico modeling or variant position)
37	c.1882C > T	p.Arg628Cys	absent	3	biallelic	NBD: disrupted intersubunit interactions
38	c.1903_1904delinsAA	p.Ala635Lys	absent	1	biallelic	NBD: disrupted intersubunit interactions
39	c.1915G > A	p.Glu639Lys	3 | 0 | 1.86e-6	2	biallelic	NBD: disrupted intersubunit interactions
40	c.1937G > T	p.Gly646Val	1 | 0 | 6.20e-7	1	biallelic	NBD: disrupted intrasubunit interactions
41	c.1937dupG	p.Cys647Leufs*26	absent	1	biallelic	NBD: disrupted intrasubunit interactions
42	c.1949G > C	p.Arg650Pro	absent	1	biallelic	NBD: disrupted intrasubunit interactions
43	c. 2045 T > A	p.Ile682Asn	absent	1	biallelic	NBD: disrupted intrasubunit interactions

Structural predictions had an even stronger association with survival than either zygosity or age of onset ($\chi^2(2) = 75.8$, $p < 0.0001$) (Fig. 2C). Genotypes predicted to result in NMD or ANK disruption were associated with the poorest outcomes compared to those with NBD variants, with median survival of 1 week for NMD and 20 months for ANK. As monoallelic cases only had variants affecting the NBD, survival outcomes in individuals with NBD-disrupting genotypes were compared across variant zygosity groups. No survival difference was observed ($p = 0.9491$), suggesting that structural impact may be more predictive than inheritance alone (Appendix A: Fig. A3b).

Univariate and multivariate regression modeling further supported these associations (Appendix A: Table A1). A multivariate model including structural disruption and age of onset retained high explanatory power (*Nagelkerke* $R^2 = 0.56$). Sex showed no significant effect and was excluded from the final model. ANK disruption (HR = 7.8, 95% CI: 3.1–20.8) and NMD genotypes (HR = 42.9, 95% CI: 11.7–175.4) were independently associated with reduced survival ($p < 0.0001$ for both), while the effect of early onset did not reach statistical significance (HR = 3.7, 95% CI: 0.9–34.0) (Fig. 2G).

3.4. Genotype and predicted structural impact correlate with disease burden (CLPB-DBI)

CLPB-DBI scores were significantly higher in biallelic cases (median [IQR]: 25 [12–27]) compared to monoallelic cases (9 [5.0–18.3]; Mann-Whitney U = 202.5, $p = 0.0002$) (Fig. 2D). Scores also differed based on variant combination and the structural disruption predicted. Individuals with stop/stop genotypes had significantly higher DBI scores than those with missense/missense (Z = 2.55, adjusted $p = 0.0324$) and missense/wild-type combinations (Z = 4.31, adjusted $p < 0.0001$) (Fig. 2E). At the structural level, NMD (Z = 3.56, adjusted $p = 0.0011$) and ANK disruptions (Z = 2.80, adjusted $p = 0.0153$) were each associated with higher disease burden than NBD-disrupting genotypes (Fig. 2F).

In univariate regression, both zygosity and structural disruption predicted DBI score (Appendix A: Table A2). In multivariate analysis, only structural disruption remained significant. NMD ($\beta = 14.4$; 95% CI: 10.8–17.8) and ANK ($\beta = 12.5$; 95% CI: 8.7–16.2) disruptions were independently associated with increased DBI (Fig. 2H). The model explained ~40% of DBI variance (adjusted *Nagelkerke* $R^2 = 0.37$; $p < 0.001$).

Exploratory variant-specific analysis, showed that individuals with the ANK variant p.Tyr272Cys ($n = 3$) had high DBI (score = 27–28) and poor survival. In contrast, those with p.Arg60 variants (n = 3) in the NBD had lower DBI (score = 5) and better survival outcomes (Fig. 2I-J).

3.5. Disease burden and progression

Based on CLPB-DBI scores, 18 individuals (7 biallelic, 11 monoallelic) had mild disease (DBI <10), 23 (13 biallelic, 10 monoallelic) had moderate disease (DBI 10–24), and 22 (21 biallelic, 1 monoallelic) had severe disease (DBI ≥ 25) (Appendix C: Table C3). A breakdown of clinical features across severity categories is provided in Table 2, with a zygosity-stratified overview in Fig. 3.

3.5.1. Symptom onset

Intrauterine growth restriction and polyhydramnios were the most frequent prenatal complications (Fig. 3A). Symptom onset occurred within the first year of life in 35/41 (85%) biallelic and 15/22 (68%) monoallelic cases, with neonatal onset in 25 (71%) and 7 (32%) respectively. Remaining cases developed symptoms between ages 1–5 years. Early signs included neutropenia and muscle tone abnormalities - ranging from generalized hypotonia, to progressive tetraspasticity and jaw lock in severe (typically biallelic) cases. Seizures, dystonia, and developmental delay typically manifested in infancy, while ataxia emerged later in early childhood. Cataracts were diagnosed in infancy in 10 biallelic individuals and between 1 and 5 years in six others; in two monoallelic cases with reported cataracts, the age of onset was not specified. Premature ovarian insufficiency, typically diagnosed between ages 13–18 years, was reported in 3/7 (43%) females with biallelic and 3/6 (50%) with monoallelic variants. Hypothyroidism occurred in 4/17 (24%) biallelic and no (0/7) monoallelic cases (Fig. 4A).

3.5.2. Phenotypic spectrum

While hematological, neurological and systemic features frequently overlapped, certain manifestations showed zygosity-related trends. Bilateral cataracts were significantly more prevalent in biallelic cases (16/29 vs 2/17, $p = 0.0047$; Fig. 3B), though no variant-specific correlations were identified. Dystonia and basal ganglia MRI signal abnormalities occurred only in biallelic individuals (12/38 vs 0, $p = 0.047$; Fig. 3D), whereas bradykinesia and ataxia were equally distributed. Brain imaging commonly revealed cerebral or cerebellar atrophy and nonspecific white-matter signal abnormalities. Recurrent infections were frequent across the cohort, but subcutaneous abscesses were significantly more common in monoallelic cases (9/21 vs 1/34, $p = 0.0004$; Fig. 3C). Among individuals where urine organic acid testing specifically included quantitation of 3-methylglutaconic acid, elevated excretion was confirmed in 38/39 (97%) with biallelic and 8/13 (57%) with monoallelic variants. Individuals with normal excretion (1 biallelic and 5 monoallelic) all had mild phenotypes (Table 2).

3.5.3. Disease progression

To assess progression, DBI scores were compared at symptom onset

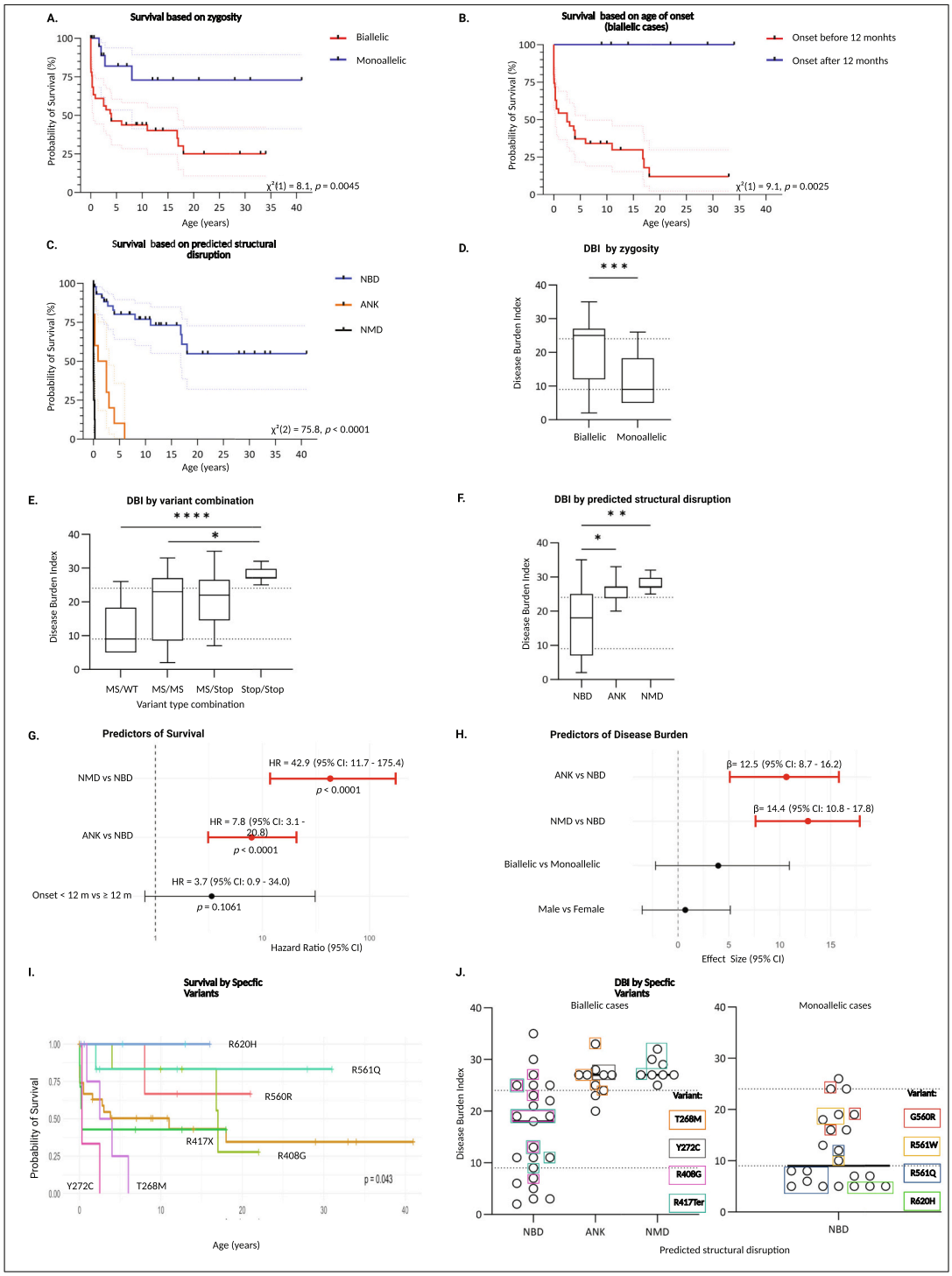

Fig. 2. Genotype–phenotype correlation analyses in CLPB-related mitochondrial disease.
(A–C) Kaplan–Meier survival curves comparing outcomes by zygosity (A), age of disease onset before vs. after 12 months (biallelic cases only) (B), and predicted structural disruption category (C). (D–F) Box-and-whisker plots showing DBI score distribution across zygosity (D), variant-type combination (E), and predicted structural disruption groups (F). Boxes represent the interquartile range, the bold horizontal line indicates median, and whiskers extend to data points with 1.5× IQR. Dashed horizontal lines indicate clinical severity cutoffs at DBI = 9 and DBI =24. (G) Forest plot of multivariate regression model assessing the independent contribution of predicted structural disruptions and age of onset to survival. Independent predictors are highlighted in red. NMD and ANK disruptions were both associated with worse survival. (H) Forest plot of multivariate regression model assessing the independent contribution of structural disruption, zygosity, and sex to DBI. Independent predictors are highlighted in red. Only NMD and ANK disruptions were independent predictors of DBI severity. (I–J) Variant-specific exploratory analyses. (I) Kaplan–Meier curves showing variant-specific survival. (J) DBI scores of individual cases across predicted disruption categories. Individuals with indicated recurrent variants are boxed for visual comparison. ANK, ankyrin repeat region, DBI, disease burden index; HR, hazard ratio; NBD, nucleotide-binding domain; NMD, nonsense-mediated decay; MS, missense; WT, wild-type; $*p < 0.05$; $**p < 0.01$; $***p < 0.001$; $****p < 0.0001$. (For interpretation of the references to colour in this figure legend, the reader is referred to the web version of this article.)

Table 2
CLPB-related mitochondrial disease phenotypes.

	Biallelic			Monoallelic	
	Mild (n = 7)	Moderate (n = 13)	Severe (n = 21)	Mild (n = 11)	Moderate/severe (n = 11)
DBI score, Median (IQR)	5 (2–7)	19 (12−22)	27 (26–30)	5 (5–7)	18 (13–24)
Deceased, n (%)	0 (0)	6 (46)	21 (100)	0	5 (46)
Age, Mean (SEM), years					
Deceased	–	3.3 (0.02–12.8)	0.3 (0.03–3.4)	–	2.4 (1.7–6.7)
Alive	18 (9–33)	12.6 (6.9–14.0)	–	29.5 (16–38.5)	9.5 (5.3–17.3)
Pregnancy complications					
Yes, # affected / # reported (%)	1/6 (17)	6/11 (55)	11/17 (65)	1/1 (100)	2/8 (25)
Hematological/Immunological					
Neutropenia					
Prevalence, # affected / # reported (%)	5/7 (71)	11/13 (85)	21/21 (100)	11/11 (100	10/11 (91)
Age at first report					
<12 m, n (%)	1 (20	6 (55)	20 (95)	5 (45)	8 (80)
≥ 12 m, n (%)	4 (80)	5 (45)	1 (5)	6 (55)	2 (20)
Recurrent infections					
Prevalence, # affected / # reported (%)	3/7 (43)	6/10 (60)	14/18 (78)	9/10 (90)	10/11 (91)
Age at first report					
<12 m, n (%)	1 (33)	5 (83)	13 (93)	NR	8 (100)
≥ 12 m, n (%)	2 (66)	1 (17)	1 (7)	NR	0
Malignancy, n	0	0	2	0	1
Neurological					
Dev. delay / Intellectual disability					
Prevalence, # affected / # reported (%)	2/7 (29)	11/11 (100)	13/18 (72)	2/8 (25)	8/9 (89)
Age at first report					
<12 m, n (%)	0 (0)	7 (64)	13 (100)	NR	4 (57)
≥ 12 m, n (%)	2 (100)	4 (36)	0 (0)	NR	3 (43)
Severity				NR	
Mild	2	4	0		2
Moderate	0	0	1		2
Severe	0	4	5		2
Profound	0	3	7		1
Regression, n	0	3	5		2
Microcephaly					
Prevalence, # affected / # reported (%)	0/5 (0)	10/11 (91)	11/12 (92)	0/4 (0)	8/10 (80)
Primary microcephaly, n (%)	0	6 (60)	7 (64)	0	3 (38)
Secondary microcephaly, n (%)	0	4 (40)	4 (36)	0	5 (62)
Seizures					
Prevalence, # affected / # reported (%)	0/7 (0)	8/11 (73)	15/21 (71)	1/9 (11)	7/11 (64)
Age at first report				NR	
<12 m, n (%)	0	1 (12)	14 (93)		3 (33)
≥ 12 m, n (%)	0	7 (88)	1 (7)		4 (67)
Status epilepticus, n	0	1	1	NR	2
Treatment, n				NR	
Single agent	0	2	1		1
Multiple agents	0	0	2		5
Refractory	0	0	2		2
Muscle tone abnormalities					
Prevalence, # affected / # reported (%)	0/7 (0)	10/11 (91)	20/20 (100)	0/4 (0)	8/10 (80
Age at first report					
<12 m, n (%)	0	8 (80)	20 (100)	0	7 (88)
≥ 12 m, n (%)	0	2 (20)	0	0	1 (12)
Hypotonia, n	0	9	11	0	7
Truncal	0	4	1	0	6
Generalized	0	5	8	0	1
Hypertonia, n	0	8	13	0	5
UL or LL spasticity	0	4	8	0	3
Progressive 4 limb spasticity	0	3	4	0	2
Dyskinetic disorders					
Prevalence, # affected / # reported (%)	0/7 (0)	8/13 (62)	13/18 (72)	0/4 (0)	3/8 (38)
Age at first report					
<12 m, n (%)	0	4 (50)	13 (100)	0	0
≥ 12 m, n (%)	0	4 (50)	0	0	3 (100)
Dystonia, n	0	4	8	0	0
Face	0	1	1	0	0
Jaw	0	1	5	0	0
Neck	0	1	3	0	0
Limbs	0	4	3	0	0
Bradykinesia	0	3	3	0	3

(*continued on next page*)

Table 2 (*continued*)

	Biallelic			Monoallelic	
	Mild (n = 7)	Moderate (*n* = 13)	Severe (*n* = 21)	Mild (*n* = 11)	Moderate/severe (n = 11)
Coordination disorders					
Prevalence, # affected / # reported (%)	1/7 (14)	4/13 (31)	3/16 (19)	0/4 (0)	3/8 (38)
Age at first report					
<12 m, n (%)	0	0	1 (33)	0	1 (33)
≥ 12 m, n (%)	1 (100)	4 (100)	2 (67)	0	2 (67)
Ataxia	0	3	2	0	1
Brain MRI or histology findings					
Atrophy (generalized or isolated)	0	6	14	0	7
Basal ganglia changes	0	3	7	0	0
White matter changes	0	5	7	0	5
Normal imaging	4	1	0	2	0
Cataracts					
Prevalence, # affected / # reported (%)	4/7 (57)	6/11 (55)	6/11 (55)	2/0 (22)	0/8 (0)
Age at first report				NR	
<12 m, n (%)	2 (50)	2 (33)	6 (100)		0
≥ 12 m, n (%)	2 (50)	4 (67)	0		0
Other systems					
Growth, # affected / # reported (%)	3/4 (75)	6/9 (67)	13/14 (93)	1/3 (33)	4/7 (57)
Endocrine, # affected / # reported (%)	2/4 (50)	3/7 (43)	1/6 (17)	2/2 (100)	1/5 (20)
Hypothyroidism	0	3	1	0	0
Premature ovarian insufficiency	2	1	0	2	1
Growth hormone insufficiency	1	1	0	1	1
Cardiac, n	1	2	3	0	0
GI/Liver, n	0	3	6	0	1
Renal, n	2	1	2	0	0
Musculoskeletal, n	0	1	3	0	1
Behavioral, n	3	0	1	0	2
3-methylglutaconic aciduria [§], n	6/7 (86)	13/13 (100)	19/19 (100)	0/5 (0)	8/8 (100)

[§] Urine organic acid testing specifically included quantitation of 3-MGA.

and last follow-up/death. Median DBI rose from 11 (IQR = 6–14) to 25 (IQR = 12–27) in biallelic cases and from 4 (IQR = 3–7) to 9 (IQR = 5–18) in monoallelic cases (Fig. 4B). In both groups, the differences in DBI at onset and follow-up reached statistical significance, with a median increase of 12 (8–14) points in biallelic cases ($p < 0.0001$) and 4.5 (2−13) in monoallelic cases ($p < 0.0001$). The rate of progression, estimated by the difference in DBI scores normalized to age, was significantly faster in biallelic (6 ± 1 points/year, 95% CI = 4–8) than monoallelic cases (1.7 ± 0.5 points/year, 95% CI = 0.7–2.7; U = 201, $p = 0.03$). The highest progression rates occurred in those with neonatal onset, particularly among biallelic individuals (8.9 ± 1.3 points/year, 95% CI = 6.3–12, $n = 25$), 15 of whom died within the first year (Fig. 4C). Among eight monoallelic individuals with neonatal onset, three died between ages 1–3 years. In contrast, disease remained mild in most patients with symptom onset after 12 months (4/6 biallelic, 6/7 monoallelic).

3.6. Developmental and functional outcomes

3.6.1. Developmental regression

Developmental delay was reported in 26/36 (72%) biallelic and 10/17 (59%) monoallelic individuals. Among affected individuals, 22/33 (67%) had severe or profound deficits. Regression occurred in 10/44 (23%) individuals – 8 biallelic and 2 monoallelic – typically within the first three years of life. Six cases (all biallelic) experienced abrupt neurologic decline in the first year of life following a period of normal development, while the remaining four individuals had preceding developmental delay. Triggers included febrile illness ($n = 5$), seizures ($n = 3$), and bone marrow transplant ($n = 1$). Affected domains included gross motor and language skills. All cases remained delayed post-regression, despite partial recovery.

3.6.2. Functional status

Across 44 individuals (36 biallelic, 8 monoallelic), 29/44 (66%) had mobility impairments, 23/34 (68%) had communication difficulties, and 20/32 (63%) required exclusive enteral feeding. Walking was achieved by 14/40 (35%) biallelic and 4/9 (44%) monoallelic individuals, while single-word use was reported in 15/40 (38%) and 5/9 (56%), respectively. Only 10–20% attained these early milestones within age-appropriate timeframes (Fig. 5A). Among ambulatory individuals, walking occurred at a mean age (±SEM) of 36 ± 10 months (biallelic, $n = 13$) and 22 ± 6 months (monoallelic, $n = 3$). First words were spoken at 14 ± 1 months (biallelic, $n = 9$) and 20 ± 3 months (monoallelic, $n = 4$). Functional impairments strongly correlated with higher CLPB-DBI scores (Fig. 5B; Appendix A: Fig. A4).

3.6.3. Outcomes in adulthood

Ten adults were included (6 biallelic, 4 monoallelic), with median ages of 25.5 years (IQR: 18–33) and 29.5 years (IQR: 24.5–36), respectively. Two presented in the neonatal period, four in infancy, and four between 1 and 5 years of age. Median DBI scores were 4 (IQR: 3–6) at presentation and 7 (IQR: 6–11) at last follow-up. One biallelic adult (ID1037) who presented in infancy had severe neurological impairment (progressive dystonia, athetosis, spasticity, intellectual disability) and died at age 18 (DBI = 18). All others had milder presentations involving neutropenia ($n = 5$) or cataracts (n = 3) and remained alive with mild or no functional limitations at last follow-up. Two individuals (ID1040 and ID1041) had successfully completed university. Thes siblings with the biallelic *CLPB* variants Arg628Cys and Glu639Lys presented with 3MGA, cataracts, and nephrocalcinosis and had normal developmental milestones in childhood [18,40].

3.7. Treatment outcomes

3.7.1. Epilepsy and anti-seizure therapy

Seizures were reported in 23/39 (59%) biallelic and 8/20 (40%) monoallelic cases. Generalized onset seizures predominated (10 biallelic, 6 monoallelic), including myoclonic ($n = 2$), tonic-clonic (n = 2),

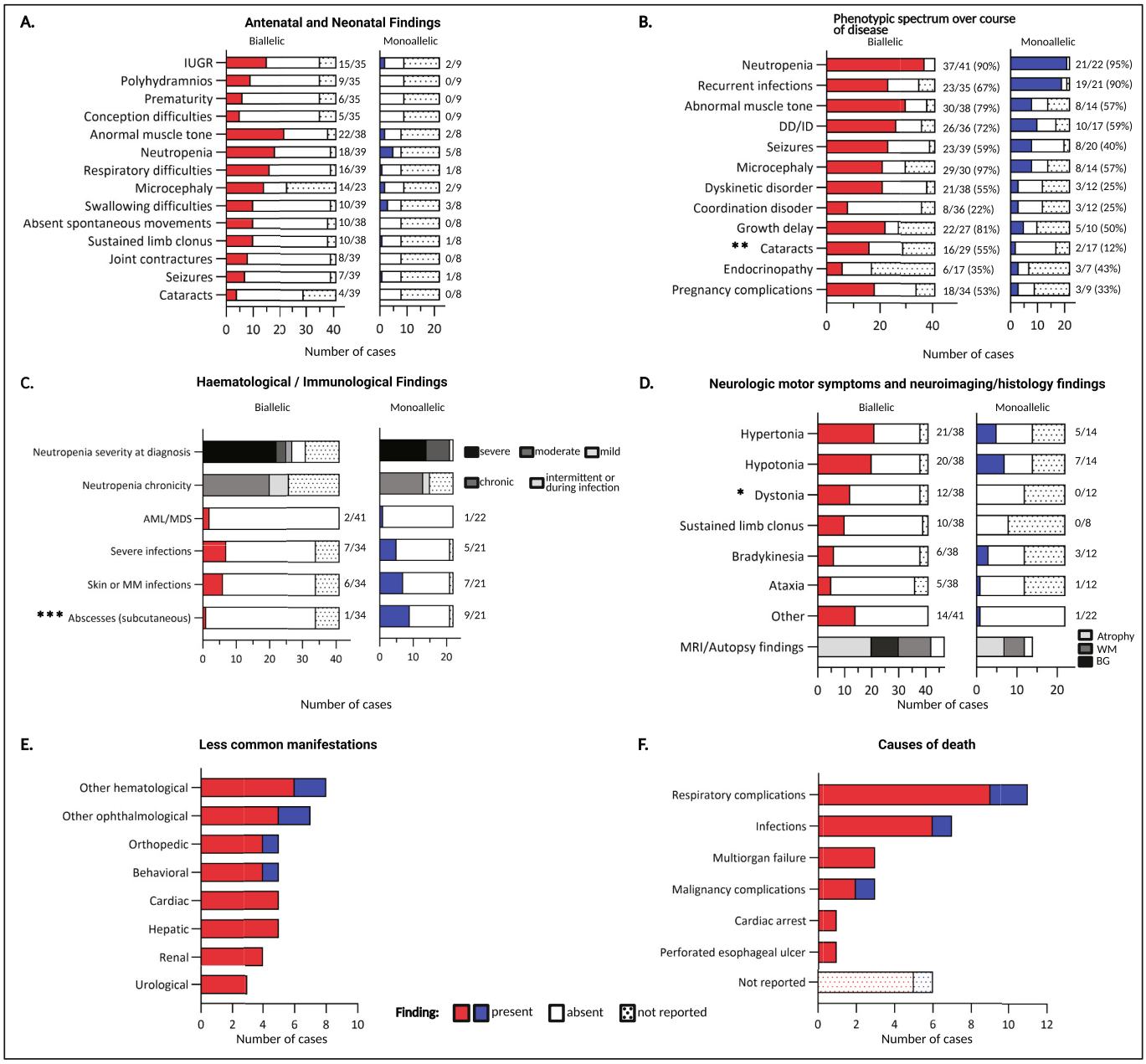

Fig. 3. Clinical characteristics of individuals with dominant (monoallelic) and recessive (biallelic) CLPB-related mitochondrial disease.
Stacked bar charts display the presence (solid colour), absence (white), or unreported status (dotted) of clinical features in individuals with biallelic (red) or monoallelic (blue) CLPB variants. Prevalence is reported as # present / # reported. (A) Antenatal and neonatal findings. Intrauterine growth restriction (IUGR) and polyhydramnios were the most frequent prenatal complications, while abnormal muscle tone was the most common neonatal feature. (B) Key phenotypic features over the course of disease, showing substantial symptom overlap across variant zygosity groups. Bilateral cataracts were significantly more common in biallelic cases ($p < 0.01$). (C) Hematological and immunological findings. Neutropenia severity is categorized as severe (ANC $< 0.5 \times 10^9$/L), moderate (0.5–0.9 $\times 10^9$/L), or mild (1.0–1.5 $\times 10^9$/L). Recurrent infections—including severe infections (sepsis, pneumonia, meningitis), mucocutaneous infections, and subcutaneous abscesses—were frequent across the cohort, but subcutaneous abscesses were significantly more common in monoallelic cases ($p < 0.001$). AML/MDS, acute myeloid leukemia/myelodysplastic syndrome. (D) Neurologic motor symptoms and findings on brain imaging/histology. Muscle tone abnormalities ranged from generalized hypotonia to progressive 4 limb spasticity and jaw lock. Dystonia and basal ganglia signal abnormalities were exclusive to biallelic cases ($p < 0.05$). Other motor symptoms included tremor, chorea, athetosis, dysarthria, and laryngopharyngeal discoordination. (E) Less common disease manifestations across various systems in biallelic (red) and monoallelic (blue) cases: hematologic (anemia, thrombocytopenia, coagulopathy), ophthalmologic (strabismus, myopia, microspherophakia), orthopedic (arthrogryposis multiplex congenita, kyphoscoliosis, clubfoot), behavioral (autism spectrum disorder, attention deficit hyperactivity disorder, impulsivity, sleep disturbance), cardiac (congenital anomalies, cardiomyopathy), hepatic (hepatomegaly, cholestasis, transaminitis), renal (nephrocalcinosis, calculi, cysts, vascular anomalies), and urologic (urogenital hypoplasia, azoospermia). (F) Reported causes of death in biallelic (red) and monoallelic (blue) cases. (For interpretation of the references to colour in this figure legend, the reader is referred to the web version of this article.)

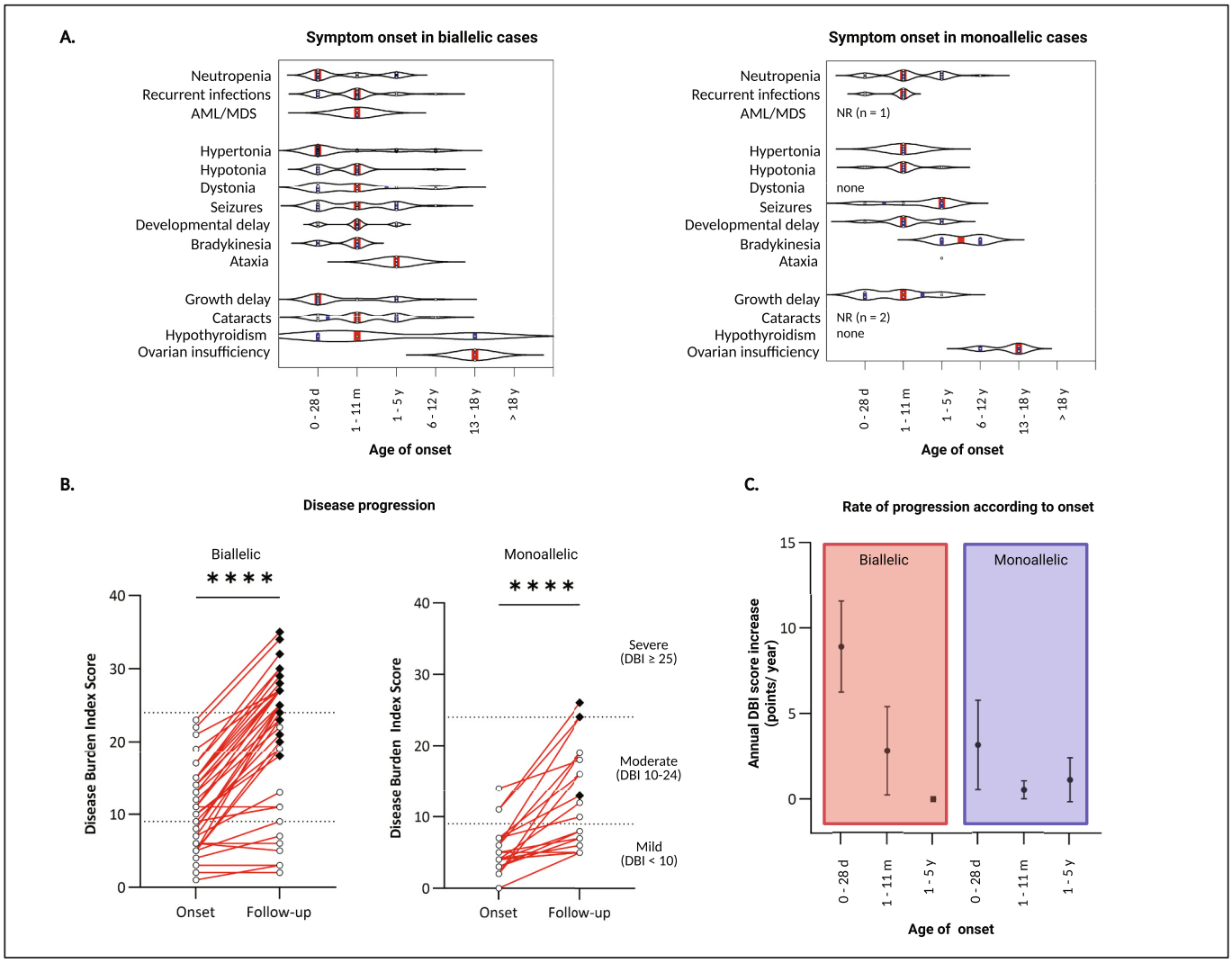

Fig. 4. Symptom onset and disease progression in individuals with CLPB-related mitochondrial disease.
(A) Age at onset (categorical) of commonest clinical features in biallelic and monoallelic cases. The median age category is highlighted in red. The age of onset of cataracts and acute myeloid leukemia/myelodysplastic syndrome (AML/MDS) in monoallelic cases were not reported (NR). (B) Vector plots comparing individual Disease Burden Index (DBI) scores at disease onset and last follow-up. Deceased individuals are indicated by black diamonds. The median DBI rose from 11 to 24 in biallelic cases (Wilcoxon signed-rank test W = 841, p < 0.0001) and from 4 to 9 in monoallelic cases (W = 252, p < 0.0001). (C) Rate of progression according to the age of disease onset. The mean annual DBI increase (= DBI follow-up - DBI onset / age) is shown, stratified by zygosity and onset categories. Error bars represent the 95% confidence interval of the mean. (For interpretation of the references to colour in this figure legend, the reader is referred to the web version of this article.)

tonic ($n = 1$), epileptic spasms (n = 1) and non-motor types (n = 2). One monoallelic case presented with focal seizures. Status epilepticus occurred in four individuals (2 biallelic, 2 monoallelic), often in the context of sepsis or following HSCT.

Treatment responses, available for 13/31 cases, varied. Two individuals had mild, self-limiting febrile seizures and myoclonic movements requiring no medication, respectively. Levetiracetam monotherapy achieved seizure control in four cases. Four others required polytherapy - including ethosuximide, cannabidiol, lacosamide, and levetiracetam – with partial benefit. Seizures were refractory in the remaining four cases; ketogenic diet was trialed in two without sustained success.

3.7.2. Neutropenia, G-CSF, and hematopoietic stem cell transplantation (HSCT)

Neutropenia affected nearly all individuals (biallelic: 37/41, 90%; monoallelic: 21/22, 95%), typically in a chronic severe form (< 0.5 × 10^9/L). Bone marrow biopsies ($n = 30$; age range at procedure 17 days – 2 years) showed myeloid maturation arrest in 27 (90%), with dysplastic or leukemic transformation in three cases (2 biallelic, 1 monoallelic). ID1063 is the only patient with monoallelic disease not to have developed neutropenia at time of follow-up, although later-onset neutropenia (at age 7 years) has previously been reported in another affected monoallelic individual (ID1050), and intermittent neutropenia might have also been missed [21].

Granulocyte colony-stimulating factor (G-CSF) was administered to 14/24 (58%) biallelic and 19/21 (90%) monoallelic neutropenic individuals, with improved neutrophil counts and fewer infections reported. G-CSF was associated with reduced mortality: 30% (10/33) vs. 67% (8/12) in untreated individuals (log-rank test $\chi^2(1) = 7.8$, $p = 0.0052$) (Appendix A: Fig. A3c). No association was observed between G-CSF therapy and leukemic transformation ($p = 0.17$).

Allogeneneic HSCT was performed in four monoallelic individuals with severe, G-CSF-refractory neutropenia (median transplant age 3.5 years [IQR: 1.6–6.5]). One died shortly post-transplant from sepsis at age 2 years (ID1043). Of the survivors, two showed improved neutrophil counts. Neurological outcomes varied. One individual (ID1049) with atypical absence seizures that developed into Lennox-Gastaut syndrome

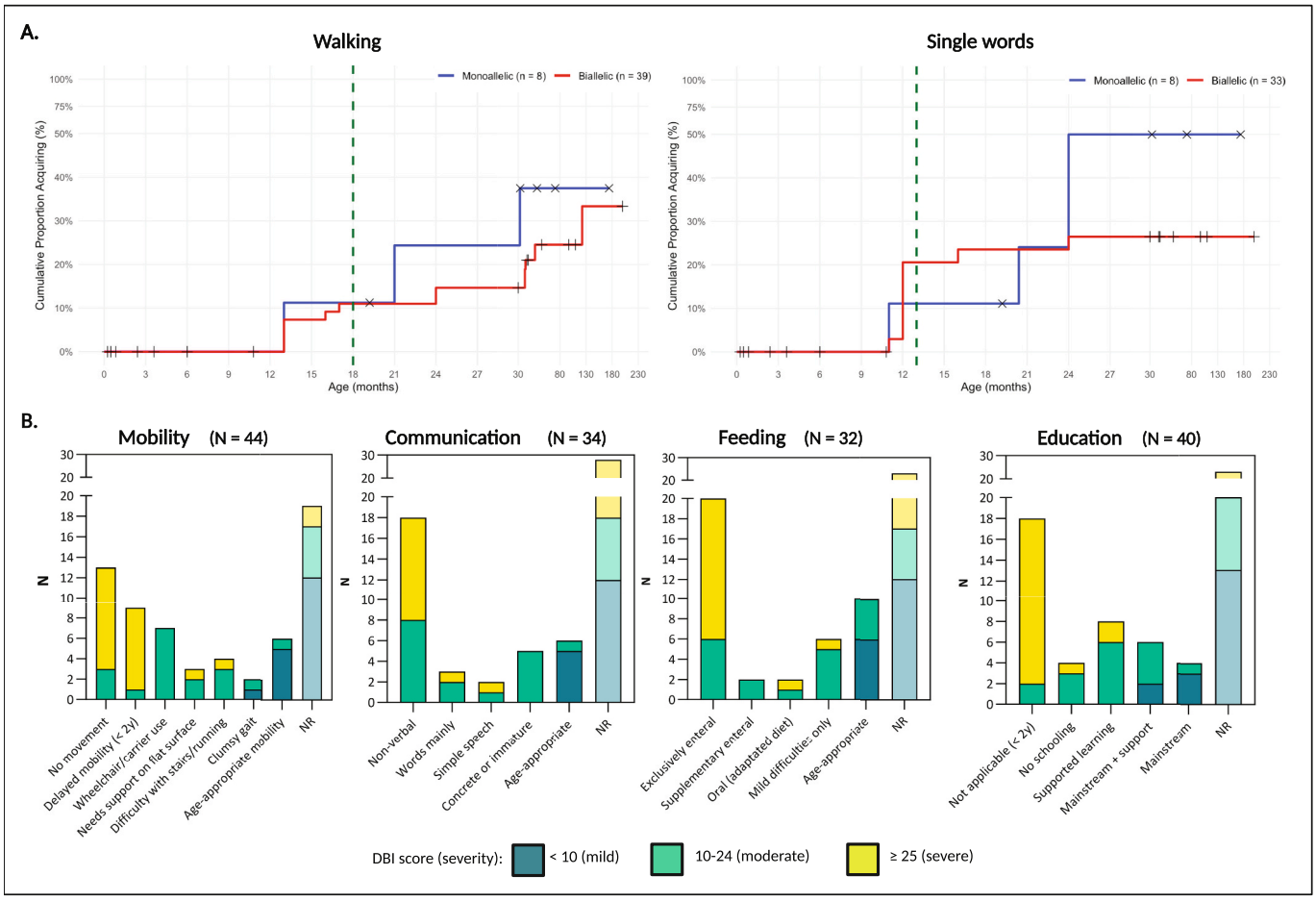

Fig. 5. Developmental and functional outcomes in individuals with CLPB-related mitochondrial disease.
(A) Inverse Kaplan–Meier curves displaying cumulative acquisition of walking and single-word speech, stratified by CLPB variant zygosity (biallelic, red; monoallelic, blue). (B) Functional outcomes pertaining to mobility, communication, feeding, and education. For each outcome, stacked bar charts show the distribution of individuals stratified by phenotype severity based on their disease burden index (DBI) score. Similar trends were observed across variant zygosity groups (Supplementary Fig. A4). (For interpretation of the references to colour in this figure legend, the reader is referred to the web version of this article.)

was transplanted at age 15 months and experienced status epilepticus post-transplant followed by motor and speech regression from the age of 22 months; at 12 years of age he can mobilise with assistance and communicates with words mainly. Another individual (ID1046) who was transplanted at 5 years old remained stable and seizure-free on levetiracetam prophylaxis 60 days post-HSCT. A third (ID1048) transplanted at age 8 years with no neurological symptoms, was reportedly well four years later.

3.7.3. Combined uridine and pyruvate (Malto-Uripyr®) supplementation

Three individuals (ID1021, ID1045, and ID1063) received oral Malto-Uripyr® supplementation over a period of 4–19 months, but this had no objective benefit on neutrophil counts or frequency of community- and hospital-managed infections (Appendix A: Detailed case reports).

4. Discussion

CLPB-related mitochondrial disease results from both biallelic and monoallelic variants, contributing to a complex clinical and genetic landscape. We present the largest cohort to date ($n = 63$) examining genotype-phenotype correlations, structural variant impact, and clinical outcomes across zygosity groups.

Biallelic disease was associated with earlier onset, higher cumulative disease burden, and reduced survival. Indeed, neonatal symptom onset, more common in individuals with biallelic variants, was associated with faster disease progression and worse prognosis, with many dying within the first year of life. These findings align with those in other progressive nuclear-encoded mitochondrial disorders such as those related to defects in *POLG* [41], *TK2* [42], or *DARS2* [43], for example, where earlier onset is associated with more severe disease and a higher mortality rate [44]. In both biallelic and monoallelic CLPB defects, most individuals who survived beyond infancy exhibited delayed motor and language development, with many (~60%) never learning to walk or to speak. It is possible that limited data availability and publication bias may have skewed our findings towards the more severe end of the phenotypic spectrum. Nevertheless, milder phenotypes with limited or no neurological involvement were also observed across inheritance patterns, and more often in individuals presenting after 12 months of age. The presence of functionally independent adults - including university-educated individuals with biallelic variants – highlights the condition's variable trajectory and the potential for favorable outcomes in milder cases. These findings support early neurodevelopmental screening and long-term multidisciplinary follow-up across all genotypes.

4.1. Structural disruption as a key predictor of disease burden and survival

In this cohort, *CLPB* variants were distinct across zygosity groups, suggesting the presence of separate pathogenic mechanisms in biallelic and monoallelic forms. Loss-of-function alleles were found exclusively in biallelic cases; missense variants predominated overall, highlighting

the protein's sensitivity to single amino acid substitutions.

Missense variants in biallelic disease were distributed throughout the gene. Structural analysis (Appendix A: Supplementary Results) suggested that many of these substitutions likely destabilize the oligomeric assembly or disrupt subunit interactions, with functional loss manifesting when both alleles are affected. By contrast, in monoallelic cases, missense variants cluster mainly within the ATP-binding pocket of the nucleotide-binding domain (NBD) and exert a dominant-negative effect [20]. This mirrors the spatial clustering of de novo missense variants with gain-of-function or dominant-negative mechanisms involved in other monogenic conditions [45–47]. Three monoallelic variants reported in this cohort (p.Pro427Leu, p.Gly429_Tyr430delinsAspAsn, and p.Lys404Thr) are located away from the ATP binding site and are predicted to affect NBD intersubunit interactions instead. Interestingly, patient ID1063 with the de novo p.Lys404Thr variant, is the only patient with monoallelic CLPB deficiency who had not developed neutropenia at the time of follow-up (7 years old). A possible structural insight into this apparently milder hematologic phenotype, is that the p.Lys404Thr variant only affects an intersubunit interaction occurring between two subunits in the CLPB hexamer, in contrast to the p.Pro427Leu and p.Gly429_Tyr430delinsAspAsn variants which affect intersubunit interactions between all subunits.

Notably, nonsense-mediated decay (NMD)-predicted and ANK-disrupting variants were the strongest predictors of disease burden and survival, surpassing zygosity alone as a prognostic factor. Unique to human CLPB, ANK mediates crucial protein-protein interactions and enables dodecamer formation via end-to-end stacking of hexamers [27,48]. While mutants unable to dodecamerize retain some disaggregase activity, they lose the capacity to refold client proteins, suggesting that dodecamerization may be essential for bridging disaggregation and refolding functions in vivo [28].

Individuals in our study with the ANK-disrupting Tyr272Cys variant had worse survival outcomes and higher DBI scores compared to those with other missense variants. Disruption at this key residue is thought to impair binding to HAX1 through formation of an intramolecular disulphide bond with Cys267 (Appendix A: Supplementary Results) [49], providing a plausible link to clinical overlap with *HAX1*-associated severe congenital neutropenia [21].

Together, these insights highlight the value of integrating structural modeling into variant interpretation, echoing its successful application in other multimeric protein disorders such as CAD deficiency [50].

4.2. Management considerations

Current treatment for *CLPB*-related disease remains largely supportive and focuses on mitigating its multisystem effects. Granulocyte colony-stimulating factor (G-CSF) remains the standard of care for severe neutropenia and was associated with improved survival in this cohort. Leukemic transformation occurred in ~5% of the cohort and was not linked to G-CSF, supporting findings in other congenital neutropenias — such as glycogen storage disease type 1b — that the leukemic risk is intrinsic to the marrow defect itself rather than therapy-induced [51,52]. Nevertheless, the age-at follow-up of this cohort may have also introduced potential bias in this regard; indeed, the risk of leukemic transformation may increase over time, as observed in other SCN syndromes [53,54].

HSCT effectively corrected hematologic abnormalities in select cases but may pose unique risks for individuals with underlying mitochondrial vulnerability. One patient developed status epilepticus and regression after HSCT, highlighting possible neurologic complications. While HSCT remains an option for G-CSF-refractory disease, careful risk–benefit assessment and close post-transplant neurologic monitoring are warranted.

Uridine-pyruvate supplementation demonstrated no benefit in three individuals, and considerable gastrointestinal side effects further reduced tolerability of the Malto-Uripyr® formulation used. Despite promising results in vitro [22], the utility of Uripyr supplementation in patients with primary mitochondrial disease remains unproven. Two individuals were already on neutropenia-modifying therapy during supplementation with Malto-Uripyr®, further compounding interpretation. For other interventions such as SGLT2 inhibitor treatment in GSD1b and G6PC3-deficiency, an important marker of efficacy for patients already on G-CSF is the ability to wean or cease G-CSF [55,56]. Here, the two patients continued to experience moderate-severe neutropenia during Malto-Uripyr® supplementation without improvement in the rate of hospital- or community-acquired infections, and so G-CSF weaning could never be attempted.

As survival improves, endocrine aspects of CLPB deficiency will require increased attention. Premature ovarian insufficiency can impact bone health, cardiovascular risk, and psychosocial well-being. Early detection allows timely hormone replacement therapy to improve long-term health and quality of life and minimize the risk of early menopause and its associated health complications [38,57]. Growth hormone insufficiency occurred in 4/24 (17%) individuals. Two patients (ID1040 and ID1053) were treated with growth hormone therapy in childhood and had a good response, with reportedly normal height in adulthood [38].

Altogether, these management insights underscore the need for multidisciplinary care strategies that address hematologic, neurologic, and endocrine complications, while highlighting the urgency for developing disease-modifying therapies.

4.3. Limitations

As a retrospective cohort assembled from diverse sources, this study is subject to limitations in data quality and follow-up. Symptom onset was recorded in broad age intervals to reduce recall bias but inevitably limited the granularity of natural history modeling. Extra-hematologic features may have been underreported in monoallelic cases from haematology-focused registries. Incomplete survival data for seven monoallelic cases may introduce uncertainty; however, we applied conservative censoring and conducted sensitivity analyses, which consistently supported the observed survival differences. The modest cohort size also limited power for some subgroup analyses, though penalized regression helped reduce potential overfitting. Moreover, the structural modeling predictions remain speculative and require further experimental validation of individual variant impact on protein domain stability. Notwithstanding these limitations, our analysis revealed important mechanistic and clinical insights.

Additionally, the CLPB Disease Burden Index (CLPB-DBI) used here builds on previous frameworks [31] and incorporates relevant clinical indicators, but its survival weighting limits its use as a prospective prognostic tool. External validation in larger, systematically followed cohorts will be essential to confirm its generalizability and refine its application in clinical practice. A CLPB-DBI calculator is provided in Appendix B to support future research and clinical application.

5. Conclusion

In summary, this study expands the current understanding of *CLPB*-related mitochondrial disease by linking genotype, structural impact, and clinical outcomes across both biallelic and monoallelic forms of the disease.

CRediT authorship contribution statement

Oliver Heath: Writing – original draft, Visualization, Validation, Project administration, Methodology, Investigation, Formal analysis, Data curation, Conceptualization. **Francisco Del Caño-Ochoa:** Writing – review & editing, Visualization, Methodology, Investigation, Formal analysis. **Safa Baris:** Writing – review & editing. **Rosalba Carrozzo:** Writing – review & editing. **David Coman:** Writing – review & editing.

Felix Distelmaier: Writing – review & editing. **Carolyn Ellaway:** Writing – review & editing. **Rene G. Feichtinger:** Writing – review & editing. **Andrea Finocchi:** Writing – review & editing. **Sergio Guerrero-Castillo:** Writing – review & editing. **Rebecca Halligan:** Writing – review & editing. **Iris Hannibal:** Writing – review & editing. **Amy Kritzer:** Writing – review & editing. **Uta Lichter-Konecki:** Writing – review & editing. **Kajus Merkevicius:** Writing – review & editing. **Bianca Panis:** Writing – review & editing. **Robert D.S. Pitceathly:** Writing – review & editing. **Chiara Pizzamiglio:** Writing – review & editing. **Katarzyna Iwanicka-Pronicka:** Writing – review & editing. **Shamima Rahman:** Writing – review & editing. **Laurie Seltzer:** Writing – review & editing. **Meinolf Siepermann:** Writing – review & editing. **Galit Tal:** Writing – review & editing. **Ron A. Wevers:** Writing – review & editing. **Szymon Ziętkiewicz:** Writing – review & editing. **Santiago Ramón-Maiques:** Writing – review & editing, Visualization, Methodology, Investigation, Formal analysis. **Johannes A. Mayr:** Writing – original draft, Visualization, Supervision, Project administration, Methodology, Formal analysis, Data curation, Conceptualization. **Saskia B. Wortmann:** Writing – original draft, Visualization, Supervision, Project administration, Methodology, Formal analysis, Data curation, Conceptualization.

Ethics

The study adhered to the tenets of the Declaration of Helsinki and received approval from the independent research ethics committee of Paracelsus Medical University, Salzburg (PMU-EK-2024-0055). Written informed consent for genetic testing was obtained from all participants or their legal guardians.

Funding

This research was funded in whole or in part by Austrian Science Fund (FWF) [I-4704-B], and by grant PID2021-128468NB-I00 financed by MCIN/AEI/10.13039/501100011033 to SR-M.

Declaration of competing interest

OH, FDC-O, SF, RC, DC, FD, CE, RGF, AF, SG-C, RH, IH, AK, UL-K, KM, BP, RDSP, CP, KI-P, SR, LS, MS, GT, RAW, SZ, SRM-M, JAM, SBW declare no competing interests.

Acknowledgements

Saskia B. Wortmann and Johannes A. Mayr are members of the European Reference Network for Rare Hereditary Metabolic Disorders (MetabERN) - Project ID No 739543. We are grateful to Prof. Gaetano-Villani (Università degli Studi di Bari Aldo Moro) for providing the Malto-Uripyr® supplement. Shamima Rahman acknowledges grant funding from Great Ormond Street Hospital Children's Charity and the National Institute of Health Research (NIHR) Great Ormond Street Hospital Biomedical Research Centre. The views expressed are those of the authors and not necessarily those of the NHS, the NIHR, or the United Kingdom Department of Health. Robert D S Pitceathly and Chiara Pizzamiglio are funded by The Lily Foundation and Muscular Dystrophy UK (MDUK). Robert D S Pitceathly is supported by a seedcorn award from the Rosetrees Trust and Stoneygate Foundation, a Medical Research Council (UK) Transition Support award (MR/X02363X/1), a Medical Research Council (UK) award (MC_PC_21046) to establish a National Mouse Genetics Network Mitochondria Cluster (MitoCluster), and the LifeArc Centre to Treat Mitochondrial Diseases (LAC-TreatMito). The University College London Hospitals/University College London Queen Square Institute of Neurology sequencing facility receives a proportion of funding from the Department of Health's National Institute for Health Research Biomedical Research Centres funding scheme. The clinical and diagnostic 'Rare Mitochondrial Disorders' Service in London is funded by the UK NHS Highly Specialised Commissioners.

Appendix A. Supplementary data

Supplementary data to this article can be found online at https://doi.org/10.1016/j.ymgme.2026.109752.

Data availability

Data will be made available upon reasonable request.

References

[1] D. Mróz, et al., CLPB deficiency, a mitochondrial chaperonopathy with neutropenia and neurological presentation, J. Inherit. Metab. Dis. 48 (3) (2025) e70025, https://doi.org/10.1002/jimd.70025 (PMID: 40194906).
[2] J.R. Hoskins, et al., Hsp90, DnaK, and ClpB collaborate in protein reactivation, Proc. Natl. Acad. Sci. USA 122 (5) (2025) e2422640122, https://doi.org/10.1073/pnas.2422640122 (PMID: 39879241).
[3] M.E. DeSantis, et al., Operational plasticity enables hsp104 to disaggregate diverse amyloid and nonamyloid clients, Cell 151 (4) (2012) 778–793, https://doi.org/10.1016/j.cell.2012.09.038 (PMID: 23141537).
[4] D. Mróz, et al., CLPB (caseinolytic peptidase B homolog), the first mitochondrial protein refoldase associated with human disease, Biochim. Biophys. Acta Gen. Subj. 1864 (4) (2020) 129512, https://doi.org/10.1016/j.bbagen.2020.129512 (PMID: 31917998).
[5] R.R. Cupo, J. Shorter, Skd3 (human ClpB) is a potent mitochondrial protein disaggregase that is inactivated by 3-methylglutaconic aciduria-linked mutations, Elife 9 (2020), https://doi.org/10.7554/eLife.55279 (PMID: 32573439).
[6] D. D'Angelo, et al., Dependence of mitochondrial calcium signalling and dynamics on the disaggregase, CLPB, Nat. Commun. 16 (1) (2025) 2810, https://doi.org/10.1038/s41467-025-57641-9 (PMID: 40118824).
[7] M.J. Baker, et al., CLPB disaggregase dysfunction impacts the functional integrity of the proteolytic SPY complex, J. Cell Biol. 223 (3) (2024), https://doi.org/10.1083/jcb.202305087 (PMID: 38270563).
[8] C. Klein, et al., HAX1 deficiency causes autosomal recessive severe congenital neutropenia (Kostmann disease), Nat. Genet. 39 (1) (2007) 86–92, https://doi.org/10.1038/ng1940 (PMID: 17187068).
[9] M. Germeshausen, et al., Novel HAX1 mutations in patients with severe congenital neutropenia reveal isoform-dependent genotype-phenotype associations, Blood 111 (10) (2008) 4954–4957, https://doi.org/10.1182/blood-2007-11-120667 (PMID: 18337561).
[10] S.B. Wortmann, et al., Inborn errors of metabolism with 3-methylglutaconic aciduria as discriminative feature: proper classification and nomenclature, J. Inherit. Metab. Dis. 36 (6) (2013) 923–928, https://doi.org/10.1007/s10545-012-9580-0 (PMID: 23296368).
[11] S.B. Wortmann, et al., 3-methylglutaconic aciduria–lessons from 50 genes and 977 patients, J. Inherit. Metab. Dis. 36 (6) (2013) 913–921, https://doi.org/10.1007/s10545-012-9579-6 (PMID: 23355087).
[12] H. Mandel, et al., Deficiency of HTRA2/Omi is associated with infantile neurodegeneration and 3-methylglutaconic aciduria, J. Med. Genet. 53 (10) (2016) 690–696, https://doi.org/10.1136/jmedgenet-2016-103922 (PMID: 27208207).
[13] M. Oláhová, et al., Pathogenic variants in HTRA2 cause an early-onset mitochondrial syndrome associated with 3-methylglutaconic aciduria, J. Inherit. Metab. Dis. 40 (1) (2017) 121–130, https://doi.org/10.1007/s10545-016-9977-2 (PMID: 27696117).
[14] R. Kovacs-Nagy, et al., HTRA2 defect: a recognizable inborn error of metabolism with 3-methylglutaconic aciduria as discriminating feature characterized by neonatal movement disorder and epilepsy-report of 11 patients, Neuropediatrics 49 (6) (2018) 373–378, https://doi.org/10.1055/s-0038-1667345 (PMID: 30114719).
[15] S.B. Wortmann, et al., CLPB mutations cause 3-methylglutaconic aciduria, progressive brain atrophy, intellectual disability, congenital neutropenia, cataracts, movement disorder, Am. J. Hum. Genet. 96 (2) (2015) 245–257, https://doi.org/10.1016/j.ajhg.2014.12.013 (PMID: 25597510).
[16] C. Saunders, et al., CLPB variants associated with autosomal-recessive mitochondrial disorder with cataract, neutropenia, epilepsy, and methylglutaconic aciduria, Am. J. Hum. Genet. 96 (2) (2015) 258–265, https://doi.org/10.1016/j.ajhg.2014.12.020 (PMID: 25597511).
[17] J.M. Capo-Chichi, et al., Disruption of CLPB is associated with congenital microcephaly, severe encephalopathy and 3-methylglutaconic aciduria, J. Med. Genet. 52 (5) (2015) 303–311, https://doi.org/10.1136/jmedgenet-2014-102952 (PMID: 25650066).
[18] M. Kanabus, et al., Bi-allelic CLPB mutations cause cataract, renal cysts, nephrocalcinosis and 3-methylglutaconic aciduria, a novel disorder of mitochondrial protein disaggregation, J. Inherit. Metab. Dis. 38 (2) (2015) 211–219, https://doi.org/10.1007/s10545-015-9813-0 (PMID: 25595726).
[19] S.B. Wortmann, et al., Neutropenia and intellectual disability are hallmarks of biallelic and de novo CLPB deficiency, Genet. Med. 23 (9) (2021) 1705–1714, https://doi.org/10.1038/s41436-021-01194-x (PMID: 34140661).

[20] J.T. Warren, et al., Heterozygous variants of CLPB are a cause of severe congenital neutropenia, Blood 139 (5) (2022) 779–791, https://doi.org/10.1182/blood.2021010762 (PMID: 34115842).
[21] Y. Fan, et al., HAX1-dependent control of mitochondrial proteostasis governs neutrophil granulocyte differentiation, J. Clin. Invest. 132 (9) (2022), https://doi.org/10.1172/jci153153 (PMID: 35499078).
[22] I. Adant, et al., Pyruvate and uridine rescue the metabolic profile of OXPHOS dysfunction, Mol. Metab. 63 (2022) 101537, https://doi.org/10.1016/j.molmet.2022.101537 (PMID: 35772644).
[23] S. Battaglia, et al., Uridine and pyruvate protect T cells' proliferative capacity from mitochondrial toxic antibiotics: a clinical pilot study, Sci. Rep. 11 (1) (2021) 12841, https://doi.org/10.1038/s41598-021-91559-8 (PMID: 34145306).
[24] S. Richards, et al., Standards and guidelines for the interpretation of sequence variants: a joint consensus recommendation of the American College of Medical Genetics and Genomics and the Association for Molecular Pathology, Genet. Med. 17 (5) (2015) 405–424, https://doi.org/10.1038/gim.2015.30 (PMID: 25741868).
[25] S.V. Tavtigian, et al., Fitting a naturally scaled point system to the ACMG/AMP variant classification guidelines, Hum. Mutat. 41 (10) (2020) 1734–1737, https://doi.org/10.1002/humu.24088 (PMID: 32720330).
[26] D. Wu, et al., Comprehensive structural characterization of the human AAA+ disaggregase CLPB in the apo- and substrate-bound states reveals a unique mode of action driven by oligomerization, PLoS Biol. 21 (2) (2023) e3001987, https://doi.org/10.1371/journal.pbio.3001987 (PMID: 36745679).
[27] R.R. Cupo, et al., Unique structural features govern the activity of a human mitochondrial AAA+ disaggregase, Skd3, Cell Rep. 40 (13) (2022) 111408, https://doi.org/10.1016/j.celrep.2022.111408 (PMID: 36170828).
[28] A. Gupta, et al., Dodecamer assembly of a metazoan AAA(+) chaperone couples substrate extraction to refolding, Sci. Adv. 9 (19) (2023) eadf5336, https://doi.org/10.1126/sciadv.adf5336 (PMID: 37163603).
[29] P. Emsley, et al., Features and development of Coot, Acta Crystallogr. D Biol. Crystallogr. 66 (Pt 4) (2010) 486–501, https://doi.org/10.1107/s0907444910007493 (PMID: 20383002).
[30] T.D. Goddard, et al., UCSF ChimeraX: meeting modern challenges in visualization and analysis, Protein Sci. 27 (1) (2018) 14–25, https://doi.org/10.1002/pro.3235 (PMID: 28710774).
[31] E. Pronicka, et al., A scoring system predicting the clinical course of CLPB defect based on the foetal and neonatal presentation of 31 patients, J. Inherit. Metab. Dis. 40 (6) (2017) 853–860, https://doi.org/10.1007/s10545-017-0057-z (PMID: 28687938).
[32] R.A. Hughes, et al., Accounting for missing data in statistical analyses: multiple imputation is not always the answer, Int. J. Epidemiol. 48 (4) (2019) 1294–1304, https://doi.org/10.1093/ije/dyz032 (PMID: 30879056).
[33] M.T. Onigbanjo, S. Feigelman, The first year, in: R.E. Behrman, R.M. Kliegman, H. B. Jenson (Eds.), Nelson Textbook of Pediatrics, Elsevier, Amsterdam, 2019, pp. 151–156.
[34] W.K. Frankenburg, et al., The Denver II: a major revision and restandardization of the Denver developmental screening test, Pediatrics 89 (1) (1992) 91–97 (PMID: 1370185).
[35] G. Villani, M. Battaglia, in: E.P. Office (Ed.), Pharmaceutical Composition Comprising Uridine and Pyruvate for Regulating the Proliferation, Activity and Survival of Immune Cells, 2022.
[36] A. Kiykim, et al., Novel CLPB mutation in a patient with 3-methylglutaconic aciduria causing severe neurological involvement and congenital neutropenia, Clin. Immunol. 165 (2016) 1–3, https://doi.org/10.1016/j.clim.2016.02.008 (PMID: 26916670).
[37] B. Rivalta, et al., Biallelic CLPB mutation associated with isolated neutropenia and 3-MGA-uria, Pediatr. Allergy Immunol. 33 (5) (2022) e13782, https://doi.org/10.1111/pai.13782 (PMID: 35616898).
[38] E.J. Tucker, et al., Premature ovarian insufficiency in CLPB deficiency: transcriptomic, proteomic and phenotypic insights, J. Clin. Endocrinol. Metab. 107 (12) (2022) 3328–3340, https://doi.org/10.1210/clinem/dgac528 (PMID: 36074910).
[39] E. Farrow, et al., Case of CLPB deficiency solved by HiFi long read genome sequencing and RNAseq, Am. J. Med. Genet. A 191 (12) (2023) 2908–2912, https://doi.org/10.1002/ajmg.a.63365 (PMID: 37548286).
[40] G.F. Laube, J.V. Leonard, W.G. van't Hoff, Nephrocalcinosis and medullary cysts in 3-methylglutaconic aciduria, Pediatr. Nephrol. 18 (7) (2003) 712–713, https://doi.org/10.1007/s00467-003-1151-z (PMID: 12750979).
[41] O. Hikmat, et al., Simplifying the clinical classification of polymerase gamma (POLG) disease based on age of onset; studies using a cohort of 155 cases, J. Inherit. Metab. Dis. 43 (4) (2020) 726–736, https://doi.org/10.1002/jimd.12211 (PMID: 32391929).
[42] C. Garone, et al., Retrospective natural history of thymidine kinase 2 deficiency, J. Med. Genet. 55 (8) (2018) 515–521, https://doi.org/10.1136/jmedgenet-2017-105012 (PMID: 29602790).
[43] L. van Berge, et al., Leukoencephalopathy with brainstem and spinal cord involvement and lactate elevation: clinical and genetic characterization and target for therapy, Brain 137 (Pt 4) (2014) 1019–1029, https://doi.org/10.1093/brain/awu026 (PMID: 24566671).
[44] N. Keshavan, S. Rahman, Natural history of mitochondrial disorders: a systematic review, Essays Biochem. 62 (3) (2018) 423–442, https://doi.org/10.1042/ebc20170108 (PMID: 29980629).
[45] T.N. Turner, et al., Proteins linked to autosomal dominant and autosomal recessive disorders harbor characteristic rare missense mutation distribution patterns, Hum. Mol. Genet. 24 (21) (2015) 5995–6002, https://doi.org/10.1093/hmg/ddv309 (PMID: 26246501).
[46] S.H. Lelieveld, et al., Spatial clustering of de novo missense mutations identifies candidate neurodevelopmental disorder-associated genes, Am. J. Hum. Genet. 101 (3) (2017) 478–484, https://doi.org/10.1016/j.ajhg.2017.08.004 (PMID: 28867141).
[47] A. Nurminen, G.A. Farnum, L.S. Kaguni, Pathogenicity in POLG syndromes: DNA polymerase gamma pathogenicity prediction server and database, BBA Clin. 7 (2017) 147–156, https://doi.org/10.1016/j.bbacli.2017.04.001 (PMID: 28480171).
[48] Z. Spaulding, et al., Human mitochondrial AAA+ ATPase SKD3/CLPB assembles into nucleotide-stabilized dodecamers, Biochem. Biophys. Res. Commun. 602 (2022) 21–26, https://doi.org/10.1016/j.bbrc.2022.02.101 (PMID: 35247700).
[49] S. Lee, et al., Structural basis of impaired disaggregase function in the oxidation-sensitive SKD3 mutant causing 3-methylglutaconic aciduria, Nat. Commun. 14 (1) (2023) 2028, https://doi.org/10.1038/s41467-023-37657-9 (PMID: 37041140).
[50] F. Del Caño-Ochoa, et al., Beyond genetics: deciphering the impact of missense variants in CAD deficiency, J. Inherit. Metab. Dis. 46 (6) (2023) 1170–1185, https://doi.org/10.1002/jimd.12667 (PMID: 37540500).
[51] J. Xia, et al., Somatic mutations and clonal hematopoiesis in congenital neutropenia, Blood 131 (4) (2018) 408–416, https://doi.org/10.1182/blood-2017-08-801985 (PMID: 29092827).
[52] D.C. Dale, et al., Neutropenia in glycogen storage disease Ib: outcomes for patients treated with granulocyte colony-stimulating factor, Curr. Opin. Hematol. 26 (1) (2019) 16–21, https://doi.org/10.1097/moh.0000000000000474 (PMID: 30451720).
[53] P.S. Rosenberg, et al., Stable long-term risk of leukaemia in patients with severe congenital neutropenia maintained on G-CSF therapy, Br. J. Haematol. 150 (2) (2010) 196–199, https://doi.org/10.1111/j.1365-2141.2010.08216.x (PMID: 20456363).
[54] J. Donadieu, et al., Analysis of risk factors for myelodysplasias, leukemias and death from infection among patients with congenital neutropenia. Experience of the French severe chronic neutropenia study group, Haematologica 90 (1) (2005) 45–53. PMID: 15642668.
[55] S.B. Wortmann, et al., Treating neutropenia and neutrophil dysfunction in glycogen storage disease type Ib with an SGLT2 inhibitor, Blood 136 (9) (2020) 1033–1043, https://doi.org/10.1182/blood.2019004465 (PMID: 32294159).
[56] S.C. Grünert, et al., Efficacy and safety of empagliflozin in glycogen storage disease type Ib: data from an international questionnaire, Genet. Med. 24 (8) (2022) 1781–1788, https://doi.org/10.1016/j.gim.2022.04.001 (PMID: 35503103).
[57] S.D. Sullivan, P.M. Sarrel, L.M. Nelson, Hormone replacement therapy in young women with primary ovarian insufficiency and early menopause, Fertil. Steril. 106 (7) (2016) 1588–1599, https://doi.org/10.1016/j.fertnstert.2016.09.046 (PMID: 27912889).